Applied Catalysis A: General 469 (2014) 306–311

Contents lists available at ScienceDirect

Applied Catalysis A: General

journal homepage: www.elsevier.com/locate/apcata

Development of highly stable catalyst for methanol synthesis from carbon dioxide

Congming Li, Xingdong Yuan, Kaoru Fujimoto*

Japan Gas Synthesis CO. LTD, 5-20, Kaigan 1-Chome, Minato-Ku, Tokyo, 105-8527, Japan

ARTICLE INFO

Article history:
Received 7 August 2013
Received in revised form 1 October 2013
Accepted 5 October 2013
Available online 15 October 2013

Keywords:
Methanol synthesis
Zr-promoted catalyst
CO_2

ABSTRACT

Zr-doped Cu-Zn-Zr-Al (CZZA) catalyst showed excellent performances for the methanol synthesis from carbon dioxide and hydrogen such as activity, selectivity and especially stability under mild conditions (such as 230 °C and 3.0 MPa). The catalyst showed excellent tolerance against water vapor. It was found that added alumina promoted the dispersion of Cu whereas it suppressed the reduction of copper oxide. On the other hand, added Zr promoted the catalytic activity of methanol synthesis from CO_2 and suppressed the inhibitive effect of water for the reaction as well as the catalyst deactivation. It was concluded that the methanol formation from CO_2 proceeds through two routes: one is the direct hydrogenation of CO_2 to methanol and another is the one which pass through the CO formation. The Zr-promoted catalyst gave methanol and CO at the selectivity ratio of 0.4 to 0.6, whereas the un-promoted catalyst gave only CO at the initial stage of the reaction. It was claimed that the doped Zr promote the in-situ reduction of oxidized Cu (which should be caused by the reaction with the co-product H_2O) by H_2 to increase the content of reduced Cu (active site) and thus the catalyst activity. The promoted reductivity of the Zr-containing catalyst prevents the crystal growth of CuO_x which cause the irreversible deactivation of catalyst.

1. Introduction

Utilization of carbon dioxide has become an important global issue due to the significant and continuous rise in CO_2 concentrations, accelerated growth in the consumption of petrified carbon-based energy in the worldwide, depletion of carbon-based energy resources [1]. Catalytic hydrogenation of carbon dioxide to produce various kinds of chemicals or fuels such as methanol or hydrocarbons has been recently considered as one of the most promising processes for the utilization of CO_2 as well as the acceptor of hydrogen [2–7]. Generally, methanol has been produced industrially from CO and H_2 containing small amount of CO_2. During the reaction, part of the CO_2 is converted to CO and H_2O. Thus, the industrially made methanol contains H_2O. However, it is not clear whether CO_2 is converted to methanol or to CO. It has been pointed out that for CO hydrogenation zero valent copper (Cu^0) is the active component [8]. Al_2O_3 has been pointed out to work as physical promoter to disperse Cu. Recently, many works concerned with the methanol synthesis from CO_2/H_2 mixture have been presented. It has been shown that Cu/Zn-based catalysts are the most useful systems for the catalytic hydrogenation of CO_2 to methanol. They are used under rather high temperature (above 250 °C) and high pressure (more than 5 MPa) and show short life time [5,9,10]. Al_2O_3 has been used often as the promoter in order to increase the stability and the activity. One of the present authors has shown that a conventional Cu/Zn/Al (CZA) catalyst showed high activity and stability for CO_2 hydrogenation when it was mixed with Pd/SiO_2, and showed that the Pd/SiO_2 acts to keep the content of Cu^0 at high level [11]. Gao et al. claims that the doped Zr promote the basicity of CZA and the adsorption of CO_2 [12]. Development of active and stable catalyst under mild reaction conditions will attract high attention from the point of the CO_2 utilizing technology. For the direct CO_2 hydrogenation, the formation of water vapor is inevitable ($CO_2 + 3H_2 \rightarrow CH_3OH + H_2O$), which inhibit the reaction strongly and leads to serious catalyst deactivation. However, little attention has been paid to elucidate the influence or to suppress its negative effects. In the present study, we will report our new findings on the effects of promoters (Al and Zr) on the methanol synthesis from CO_2 hydrogenation. Also, the promotive effects of Zr on the catalysis are analyzed from the relationship between the structure and the reaction performances. The Zr oxide doped Cu-Zn based catalyst was prepared by a simple co-precipitation method.

2. Experimental

2.1. Catalyst preparation

The investigated catalysts were prepared by a conventional co-precipitation method. It was precipitated from

* Corresponding author. Tel.: +81 695 3202; fax: +81 695 3309.
E-mail address: fujimoto070@gmail.com (K. Fujimoto).

0926-860X/$ – see front matter © 2013 Published by Elsevier B.V.
http://dx.doi.org/10.1016/j.apcata.2013.10.010

an aqueous solution of $Cu(NO_3)_2{\cdot}3H_2O$, $Zn(NO_3)_2{\cdot}6H_2O$, $ZrO(NO_3)_2{\cdot}2H_2O$, $Al(NO_3)_3{\cdot}9H_2O$ (all Wako, total cation concentration 1 M) by dropwise addition of a 1 M aqueous solution of Na_2CO_3 at 65 °C to final pH of 7. The precipitate was then filtered, dried, and then calcined in air at 400 °C for 5 h. The resulting catalyst has the composition of CZA ($Cu/ZnO/Al_2O_3$ = 4/3/3), CZZA ($Cu/ZnO/ZrO_2/Al_2O_3$ = 4/3/1.5/1.5), CZZ ($Cu/ZnO/ZrO_2$ = 4/3/3) by weight. Finally, the resultant powder was shaped into granules and to 20–40 meshes for the reaction.

2.2. Catalyst characterization

XRD patterns of catalyst samples were measured under ambient atmosphere with a RIGAKU X-ray diffract meter equipped with a Cu *K*α radiation. The specific surface area of the catalysts was determined by BET method using a Micromeritics ASAP 2010. X-ray photoelectron spectra (XPS) of the calcined catalysts were recorded on an ESCALAB 250 spectrometer using Al *K*α radiation (1486.6 eV). The binding energies were calculated with respect to C 1s peak at 284.6 eV.

TPR carried out with a BELCAT-B instrument. The sample (50 mg) was previously treated in He flow up to 350 °C and kept for 2 h followed by cooling to 50 °C. The 10% H_2/He mixture was passed over samples at a flow rate of 30 ml/min with a heating rate of 10 °C/min up to 400 °C. The effluent gas was passed over a molecular sieve trap to remove the generated water and then analyzed by GC equipped with TCD.

The surface of Cu metal number was measured by N_2O titration method by using the same BELCAT-B instrument. Prior to titration, the sample with about 50 mg was reduced at 250 °C for 2 h with 10% H_2/He flow, followed by purging and cooling with He flow to 50 °C. The consumption of N_2O as well as the evolution of N_2 on the metallic Cu sites ($2Cu + N_2O \rightarrow Cu_2O + N_2$) was measured at 50 °C by a thermal conductivity detector (TCD). The surface area of metallic Cu was calculated by assuming 1.46×10^{19} Cu atoms/m^2 and N_2O/Cu molar stoichiometry of 0.5 and the particle size of Cu was calculated with the equation of 6000/(8.92 × Cu metal surface area/Cu fraction in gram catalyst) [13,14].

2.3. Procedures for catalytic reaction and product analysis

A pressurized flow type reaction apparatus with a fixed-bed reactor was used for this study. The apparatus was equipped with an electronic temperature controller for a furnace, a tubular reactor with an inner diameter of 8 mm, thermal mass flow controllers for gas flows and a back-pressure regulator. A thermocouple was set at the axial center of the tubular reactor. One gram of catalyst was placed in the reactor with inert quartz sands above and under the catalyst. All catalysts were reduced in the flow of 5% H_2 in nitrogen at 250 °C for 4 h before reaction. All the products from the reactor were analyzed by on line gas chromatograph (GC).

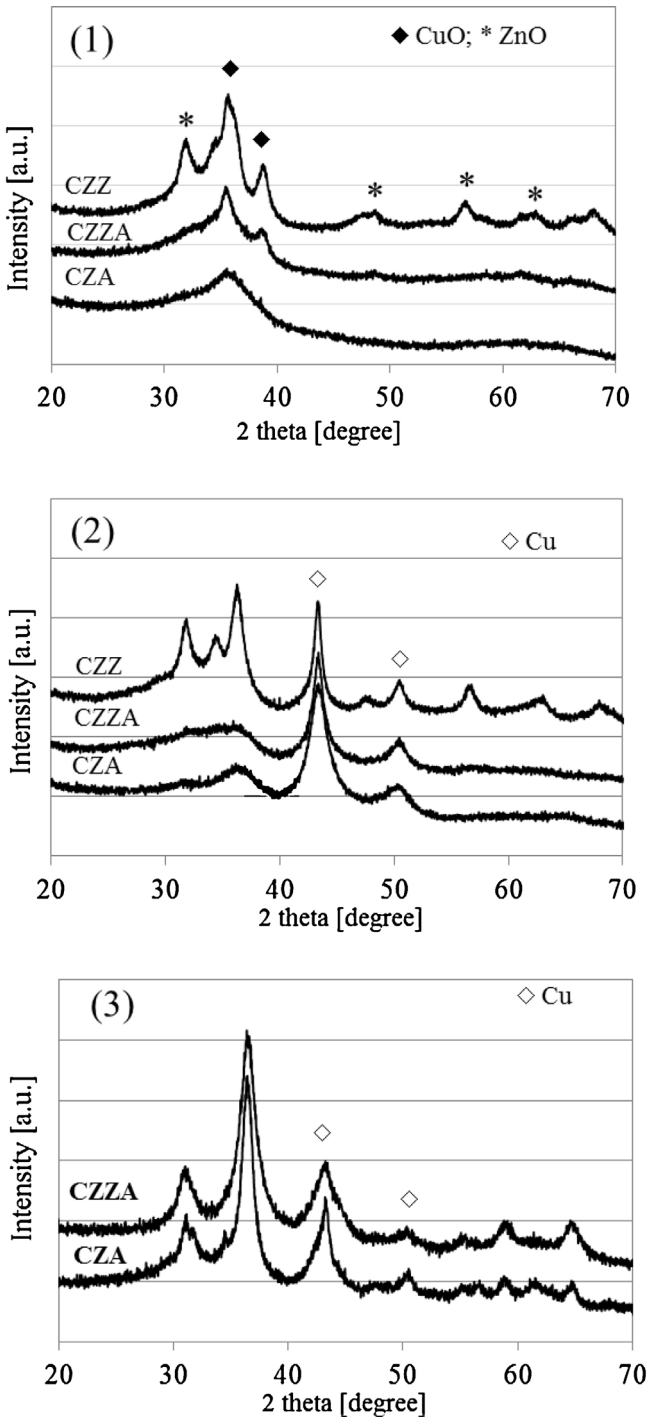

Fig. 1. XRD patters of catalysts: (1) calcined; (2) reduced and (3) after 100 h reaction.

3. Results and discussion

3.1. Catalyst structure and their character

3.1.1. Structure

The XRD patterns of (1) calcined, (2) reduced and (3) used catalysts are shown in Fig. 1. Results obtained suggest the presence of a CuO phase (2θ = 35.5°, 38.5°) for calcined samples. In addition to these peaks, there also appeared peaks that were assigned to ZnO at 31.8°, 48°, 56.6°, 62.8°, 68° for CZZ sample, which is agreed well with that obtained by Wang [15]. After reduction, the peaks at 43° and 50° were attributed to metallic Cu, which performed as a role as active component for methanol synthesis [16,17]. Using Debye–Scherrer Formula, the crystallite sizes of Cu are calculated as 8.8 nm in CZA, 9.4 nm in CZZA and 12.5 nm in CZZ, respectively.

The crystallite size growth of Cu occurred as well as CuO during stability test, which could be estimated to be 11.4 nm for CZZA and 13.8 nm for CZA, respectively, implying the significant negative effect of crystal growth in the CO_2 hydrogenation.

Table 1
Characters of Cu/ZnO-based catalysts for methanol synthesis.

Cat	BET (m^2/g)	Pore volume (cm^3/g)	Pore diameter (nm)
C	9.8	0.11	
CZ	29.8	0.40	55.8
CZA	78.3	0.35	29.5
CZZA	106.3	0.54	16.6
CZZ	90.9	0.44	16.6

3.1.2. Specific surface area and Cu surface

The data on BET surface area, pore volume and average diameter of the calcined catalysts are shown in Table 1. It can be observed that without the addition of alumina, even after Zn promotion, the CZ (CuO/ZnO) catalyst shows very low surface area of 29.8 m^2/g. It is also found from Table 1 that the surface area of the CZZA catalyst is significantly higher than the catalyst promoted on either Al_2O_3 or ZrO_2. It can be observed that the CZZA catalyst exhibits the highest surface area of 106.3 m^2/g, and CZZ (90.9 m^2/g) and CZA (78.3 m^2/g) followed. Similar trends are also observed in the pore volume data from BET. These results reiterate the role of Al_2O_3 as a structure promoter in providing a highly dispersed CuO/ZnO structure. The increase in surface area of CZZA is possibly attributed to further enhancement by the simultaneous addition of Zr, implying the same addition of Al_2O_3 and ZrO_2 increases the total surface area.

The Cu surface areas and Cu dispersions of the reduced samples, measured by N_2O titration, are shown in Table 2. Interestingly, the aluminum-containing catalyst (CZA) had the highest Cu surface area. It is likely that the sintering of Cu in CZZA occurred during the initial reduction, to decrease the Cu surface areas compared to that in CZZ [18].

3.1.3. Reducibility of CuO

The TPR profiles of the calcined samples, along with those of pure CuO and CuO/ZnO prepared with a nominal composition of 40/30 (wt%) as reference catalysts, are given in Fig. 2. The TPR profile of the calcined CuO sample (C) shows mainly one reduction peak at around 250°C, which was assigned to the reduction of $CuO \rightarrow Cu$ or $CuO \rightarrow Cu_2O \rightarrow Cu$. Although the reduction of zinc oxide is thermodynamically feasible at high temperatures, it was not reduced under the experimental conditions described here [19]. The presence of one peak in the TPR profile of CuO/ZnO (CZ) is in accordance with the literature reported previously [20–22]. The reduction peak of the CuO/ZnO catalyst was shifted by almost 50 °C toward lower temperature in comparison to that of the CuO reference catalyst, implying that the presence of zinc oxide enhances the reducibility of the copper oxide phase, and this fact agrees with previous observations [19].

The addition of Al_2O_3 to CZ catalyst exhibited two broad reduction peaks, and the second peak centered at 250 °C made the shift of reduction peak to higher temperature by about 50 °C compared with CZ catalyst. The results indicate that the presence of zinc oxide enhances the reducibility of the copper oxide phase. As to the CZA, the reduction peak obviously shifted to high temperature even though the dispersion CuO on CZA is higher than that on CZZA, which was ascribe to the strong interaction between Al_2O_3 and CuO.

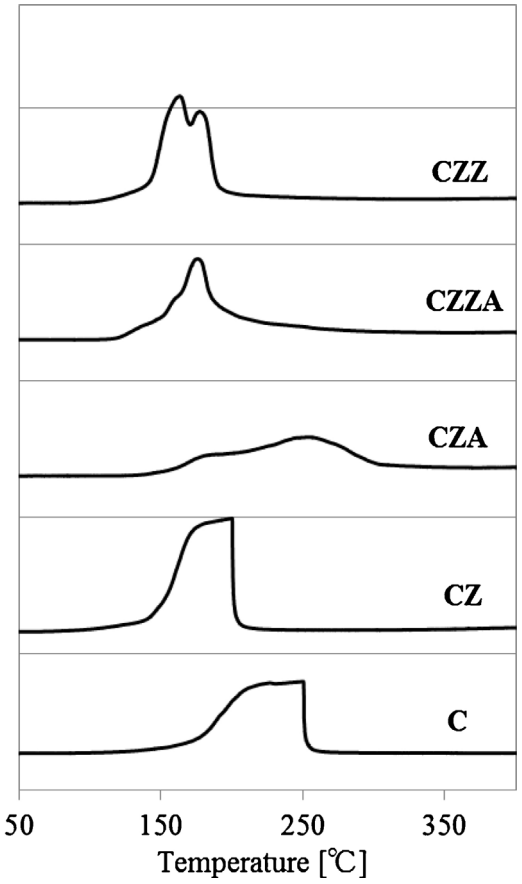

Fig. 2. TPR profiles of calcined catalysts.

However, the reduction peak of CZZA is by about 75 °C lower than that of CZA and even lower than that of CuO/ZnO. Also, it should be noted that the addition of ZrO_2 to CuO/ZnO lower the reduction temperature by about 30 °C. All these phenomena suggest that the added Al_2O_3 promotes the CuO dispersion and suppresses its reduction probably because of the small crystal, whereas the added ZrO_2 in CuO/ZnO-based catalyst promote the reduction of CuO.

Table 2
N_2O chemisorption data for calcined catalyst.

Catalysts	Surface area of copper (m^2/g)	Metallic copper particle size (nm)[a]	D_m (%)[b]
CZA	17.8	12.0	8.6
CZZA	17.4	12.3	8.5
CZZ	16.8	12.8	8.2

[a] The particle size of Cu was calculated by using the equation of 6000/(8.92 × Cu metal surface/Cu fraction in gram catalyst).
[b] Copper dispersion: D_m = exposed copper atoms/total copper atoms.

3.1.4. Electronic state

The chemical state of the calcined catalysts was evaluated by XPS (Fig. 3). The XPS spectra of the calcined samples, CZA, CZZA and CZZ show that the Cu 2p3/2 and Cu 2p1/2 peaks appeared at 933.0, 952.7; 932.7, 952.7; 933.1, 952.7 eV, respectively, which were the characteristics peaks of Cu^{2+} species [23,24]. Furthermore, the presence of peak appearing at ca. 942.0 eV evidenced the presence of Cu^{2+} ions in the form of cupric oxide [25]. The binding energies of Cu 2p3/2 and Cu 2p1/2 of the calcined catalysts were different, revealing that the chemical state of CuO was influenced by the composition of the catalyst, i.e., the electron density surrounding Cu atom was changed with the addition of alumina and/or zirconia.

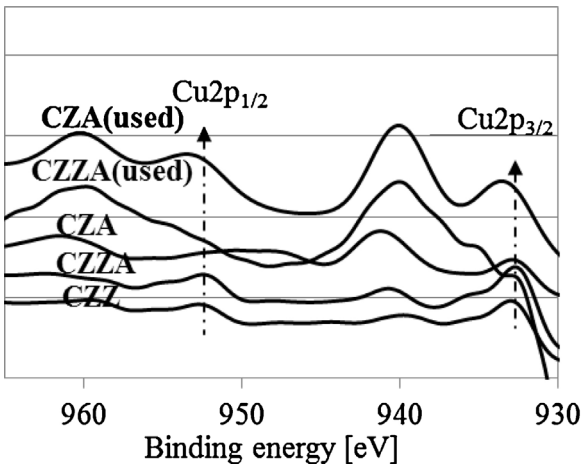

Fig. 3. XPS spectra of calcined and used catalysts (after stability test).

3.2. Catalytic performance

3.2.1. General features of CO_2 hydrogenation over Cu/ZnO-based catalysts

When a mixture of CO_2/H_2 was contacted with Cu/ZnO-based catalysts at the operating conditions described above, the main products of the reaction were methanol, CO and water. Methane was not detected as the significant byproduct.

3.2.2. Reaction performance of Cu/ZnO-based multicomponent catalysts

The catalytic activity and selectivity of methanol on three catalysts are listed in Table 3, which show results of methanol synthesis reaction at 230 °C and 3 MPa for 20 h. Conversion of CO_2 and methanol yield were a little higher on CZZA compared to those on CZA and CZZ. The selectivity of methanol on CZZA was by 17.3% higher than that on CZA, 11.7% higher than that on CZZ. Obviously, the copper surface area alone cannot explain the catalytic behavior of the catalyst. These findings indicate that the promoting effect of ZrO_2 is exerted in the catalyst. First, it is probably due to the higher dispersion of CuO particles in the Al_2O_3-ZrO_2 promoted catalyst, which provides a larger reactive surface area and, therefore, a high activity. It can be seen that there is apparent correlation between the surface area and the catalytic activity. It is noted that the conversion of CO_2 increases with increase of surface area as shown in Tables 1 and 3. The Al_2O_3-ZrO_2-promoted catalysts were found to exhibit better catalytic properties than the catalyst supported on either Al_2O_3 or ZrO_2 alone. This phenomenon will be discussed later.

Another excellent property is that the catalytic activity of CZZA is much more stable than that of CZA. The advantage of using Al_2O_3-ZrO_2 as catalyst promoter was investigated by other researchers [26–30]. These advantages include a high surface area, basicity, and thermal stability, etc. by a combination of both the supports in a mixed oxide. In Fig. 6 are shown the performance of CZA, CZZ and CZZA for the CO_2 hydrogenation as function of W/F. It showed that at high W/F (long contact time), all of them show similar CO_2 conversion and product selectivity, which are close to that equilibrium data. However, in the range of short contact time, performances of these catalyst showed quite different features, which will be discussed in the part of Section 3.

Table 3
Reaction performance of different methanol synthesis catalysts.

Cat.	CO_2 Conv. (%)	Methanol productivity (mol/h/kg)	Methanol Selectivity (%)
CZA	18.7	2.15	43.0
CZZA	23.2	3.75	60.3
CZZ	19.3	2.51	48.6

Reaction conditions: 3 MPa; 230 °C; H_2/CO_2 = 3/1, W/F = 10 g cat h/mol.

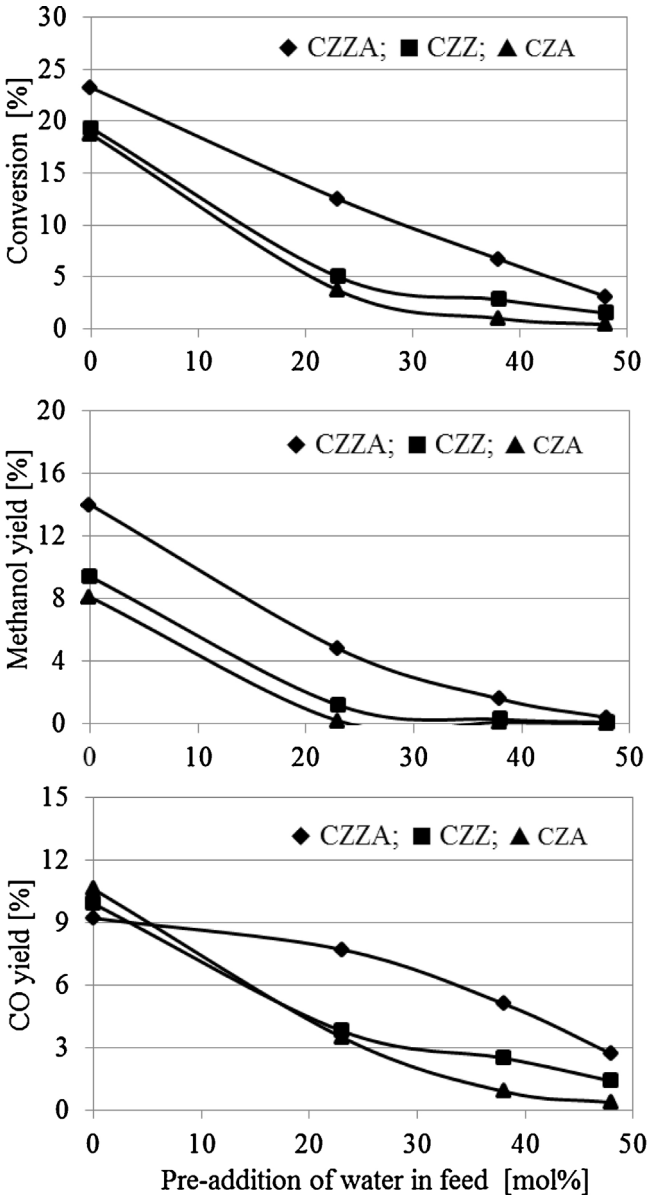

Fig. 4. Influence of pre-addition of water.

3.2.3. Influence of water

Taking into account that the equi-molar amount of water, produced during the hydrogenation of CO_2, it must affect the performances of Cu-Zn based catalyst. The poisoning effect of added water for CO_2 hydrogenation was carried out. The curve with the pre-addition of water was shown in Fig. 4. It was noted that when water was added in the experiment, the conversion immediately decreased to reach a steady state level depending on the amount of water used. The activity was recovered slowly to the original level when the water supply was stopped. The results suggested that water temporally poison the active site of the catalyst and suppress the methanol formation. It is also noted that the addition of water have a promotion effect on the CO selectivity from reversed water gas shift reaction even under the case of serious deactivation. Over the investigated catalysts, CZZA is proved to be the most resistant

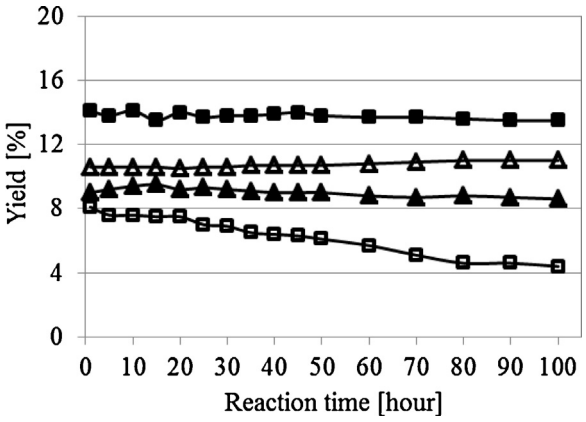

Fig. 5. Stability of CZZA and CZA catalyst: CZZA: (■) CH_3OH yield, (▲) CO yield; CZA: (□) CH_3OH yield. (△) CO yield: test conditions: 3.0 MPa, 230 °C, H_2/CO_2 = 3, W/F = 10 g cat h/mol.

against water poisoning. Similar trends were also observed when the concentration of water was increased. It should be noted that the suppressive effect is most remarkably for CZA and lowest for CZZA.

3.2.4. Stability

An important aspect of the catalyst is stability during the process of reaction. As shown in Fig. 5, CZZA catalyst keep a constant methanol synthesis activity and CO formation activity over almost 100 h, whereas CZA showed gradual decrease in methanol synthesis activity from 8.1% at 1 h to 4.4% at 100 h while keeping CO formation almost constant. The marked effects of the ZrO_2 to CZA catalyst will be discussed, later. This suggested that water produced would account for the poorer performance of Al_2O_3-promoted catalyst in CO_2 feedstock compared with ZrO_2-Al_2O_3 promoted system, which is in good agreement with the results obtained from the influence of water as shown in Fig. 4.

The XRD data in Fig. 1 suggest that the size of crystal of Cu after H_2 reduction is smaller for CZA but become larger after 100 h reaction compared to CZZA. The peak attributed to CuO was observed at 36.4° after reaction, suggesting part Cu was again oxidized during the reaction. A small peak attributed to tetragonal ZrO_2 appeared at 30.9° in the patter for CZA and CZZA after stability test (Fig. 4(3)) [31]. The crystallite size of Cu for CZZA after 100 h was 11.4 nm and significantly smaller than that for CZA.

Fig. 3 also shows the XPS results of the used catalyst CZZA and CZA after stability test. It was noted that the main Cu 2p3/2 peak of used CZA shifted toward higher binding energies compared with used CZZA, which is attributed to Cu^{2+} in a CuO environment and indicated that CZA is easy oxidized in the reaction leading to larger crystallite size [19]. This result is good agreement with that obtained by XRD and catalytic test.

3.2.5. Discussion on the promotional effect of ZrO_2 on the CO_2 hydrogenation

In order to clarify whether methanol is produced indirectly via the intermediate formation of carbon monoxide and then hydrogenation or directly by the carbon dioxide hydrogenation, the influence of the space velocity on the methanol selectivity was investigated (as shown in Figs. 6 and 7). It is interesting to note that methanol and carbon monoxide can be formed via simultaneously particularly at short contact time for CZZA compared with that shown for CZZ and CZA. The results indicate the activation of carbon dioxide to methanol by CZZA pass through two parallel routes: one is the direct process from CO_2 and another is the one which pass through CO (as

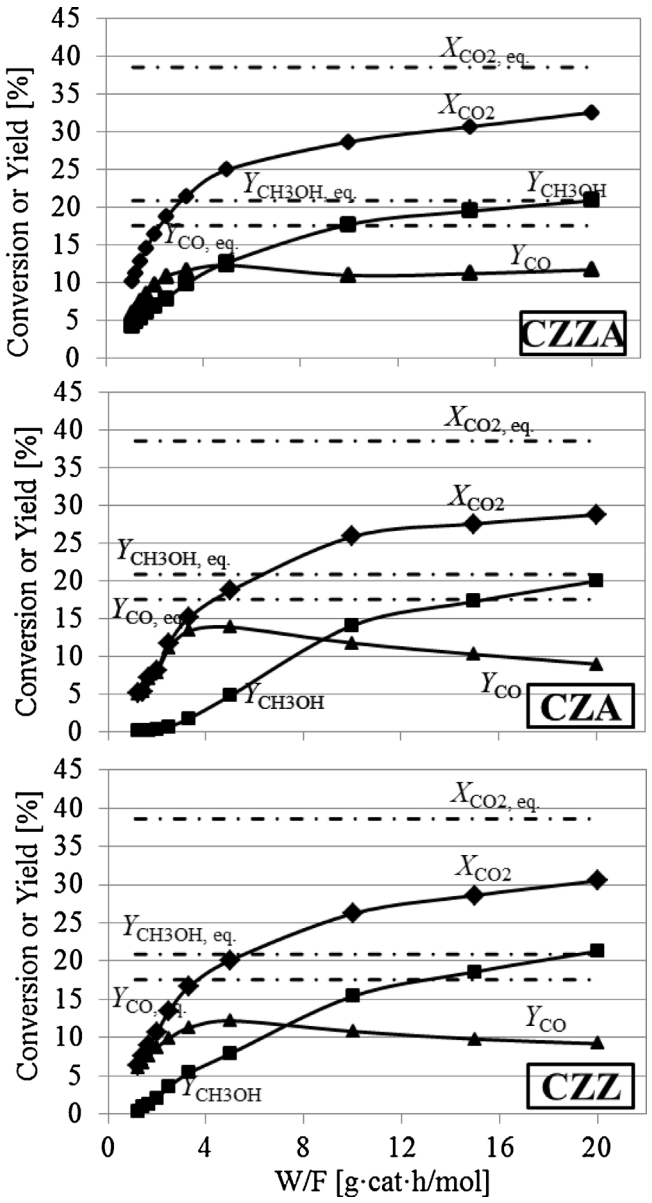

Fig. 6. Effect of W/F: test conditions: 3.0 MPa, 230 °C, H_2/CO_2 = 5.

shown in Fig. 8). While the initial product is only CO, and the methanol formation start after CO formation for CZA and CZZ.

During CO_2 hydrogenation, equi-molar amount of water is inevitably produced ($CO_2 + 3H_2 \rightarrow CH_3OH + H_2O$, $CO_2 + H_2 \rightarrow CO + H_2O$). It is well known that water is strong oxidant at high temperature for metals such as copper ($Cu + H_2O \rightarrow CuO + H_2$), Co for Fischer–Tropsch reaction. Therefore, the methanol synthesis catalyst is easy to lose its activity because of the oxidation of active site. The oxidized (CuO_x) can be reduced by hydrogen gas or CO ($CuO_x + H_2 \rightarrow Cu + xH_2O$, $CuO_x + CO \rightarrow Cu + CO_2$). However, when its rate is not high enough, most of the active site is oxidized to lose its activity. As shown in Fig. 1, the crystallite size of Cu^0 of CZA obviously increased after 100 h stability test. On the contrary, the added Zr ion apparently promotes the reduction of catalyst by hydrogen as indicated from the data in Fig. 2, suggesting that the rate of reduction of CuO is higher for CZZA than that of CZA, which are also well interpreted by the results of XRD. The phenomenon could be the reason of the higher catalytic stability for CO_2 conversion to methanol.

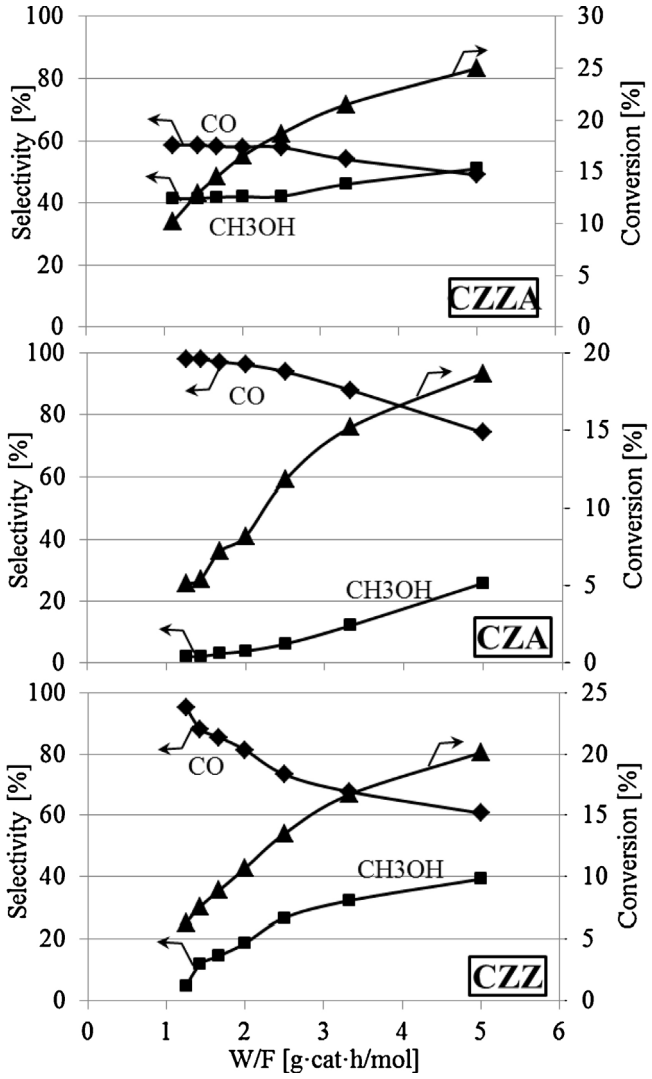

Fig. 7. Effect of *W*/*F* on selectivity.

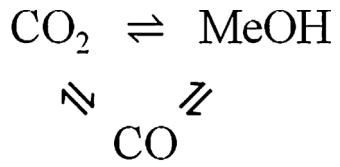

Fig. 8. Reaction path of CO_2 hydrogenation to CH_3OH over CZZA.

4. Conclusions

It is concluded that, the doped Zr in Cu-Zn based catalyst promoted the hydrogen reduction of oxidized Cu surface, generated by water vapor to increase the concentration of metallic Cu, which is the active site for the methanol formation. The methanol formation from CO_2 over CZZA was assumed to pass through two routes: one is the direct hydrogenation of CO_2 to methanol, another is the route which pass through CO formation, while the route which pass through the CO formation is only route on CZA. The promoted stability of CZZA in CO_2 hydrogenation could be attributed to the promoted reduction of copper oxide, by added zirconium, which is formed through the oxidation by water vapor, and makes larger CuO crystal.

Acknowledgments

This work was supported by New Energy and Industrial Technology Development Organization (NEDO).

References

[1] C.S. Song, Catal. Today 115 (2006) 2–32.
[2] L. Fan, K. Fujimoto, Energy Convers. Manage. 36 (1995) 633–636.
[3] K. Fujimoto, T. Shikada, Appl. Catal. 31 (1987) 13–23.
[4] J. Toyir, P.R. Piscina, J.L.G. Fierro, N. Homs, Appl. Catal., B 29 (2001) 207–215.
[5] C. Yang, Z.Y. Ma, N. Zhao, W. Wei, T.D. Hu, Y.H. Sun, Catal. Today 115 (2006) 222–227.
[6] J. Wambach, A. Baiker, A. Wokaun, Phys. Chem. Chem. Phys. 1 (1999) 5071–5080.
[7] H.W. Lim, M.J. Park, S.H. Kang, H.J. Chae, J.W. Bae, K.W. Jun, Ind. Eng. Chem. Res. 48 (2009) 10448–10455.
[8] K. Klier, V. Chatikavanij, R.G. Herman, G.W. Simmons, J. Catal. 74 (1982) 343–360.
[9] G.C. Chinchen, P.J. Denny, J.R. Jennings, M.S. Spencer, K.C. Waugh, Appl. Catal. 36 (1988) 1–65.
[10] J.C.J. Bart, R.P.A. Sneeden, Catal. Today 2 (1987) 1–124.
[11] K. Fujimoto, Y. Yu, Stud. Surf. Sci. Catal. 77 (1993) 393–396.
[12] P. Gao, F. Li, H.J. Zhan, N. Zhao, F.K. Xiao, W. Wei, A.S. Zhong, H. Wang, Y.H. Sun, K. Fujimoto, Y. Yu, J. Catal. 298 (2013) 51–60.
[13] J.W. Evans, M.S. Wainwright, A.J. Bridgewater, D.J. Yong, Appl. Catal. 7 (1983) 75–83.
[14] J.W. Bae, S.H. Kang, Y.J. Lee, K.W. Jun, Appl. Catal., B 90 (2009) 426–435.
[15] X. An, J.L. Li, Y.Z. Zuo, Q. Zhang, D.Z. Wang, J.F. Wang, Catal. Lett. 118 (2007) 264–269.
[16] J. Yoshihara, C.T. Campbell, J. Catal. 161 (1996) 776–782.
[17] C. Yang, C.A. Mims, R.S. Disselkamp, J.H. Kwak, C.H. FerricPeden, C.T. Campbell, J. Phys. Chem. C 114 (2010) 17205–17211.
[18] P.H. Matter, D.J. Braden, U.S. Ozkan, Catal. J. 223 (2004) 340–351.
[19] I.M. Cabrera, M.L. Granados, J.L.G. Fierro, J. Catal. 210 (2002) 285–294.
[20] G. Fierro, M. Lo Jacono, M. Inversi, P. Porta, F. Cioci, R. Lavecchia, Appl. Catal., A 137 (1996) 327–348.
[21] T.H. Fleisch, R.L. Mieville, J. Catal. 90 (1984) 165–172.
[22] A.L. Boyce, P.A. Sermon, M.S.W. Vong, M.A. Yate, React. Kinet. Catal. Lett. 44 (1991) 309–319.
[23] R.T. Figueiredo, M. Arias, M.L. Granados, J.L.G. Fierro, J. Catal. 178 (1998) 146–152.
[24] Y.H. Feng, H.B. Yin, A.L. Wang, L.Q. Shen, L.B. Yu, T.S. Jiang, Chem. Eng. J. 168 (2011) 403–412.
[25] C.L. Aravinda, P. Bera, V. Jayaram, A.K. Sharma, S.M. Mayanna, Mater. Res. Bull. 37 (2002) 397–405.
[26] J.M. Dominguez, J.L. Hernandez, G. Sandoval, Appl. Catal., A 197 (2000) 119–130.
[27] J.L. Lakshmi, T.R.B. Jones, M. Gurgi, J.M. Miller, J. Mol. Catal. A: Chem. 152 (2000) 99–110.
[28] K.V.R. Chary, C.P. Kumar, P.V.R. Rao, V.V. Rao, Catal Commun. 5 (2004) 479–484.
[29] K.V.R. Chary, C.P. Kumar, D. Naresh, T. Bhaskar, Y. Sakata, J. Mol. Catal. 243 (2006) 149–157.
[30] M. Moran-Pineda, S. Castillo, T. Lopez, R. Gomez, C. Borboa, O. Novaro, Appl. Catal., B 21 (1999) 79–88.
[31] Y. Matsumura, H. Ishibe, J. Mol. Catal. A: Chem. 345 (2011) 44–53.